JOURNAL OF CATALYSIS 125, 157–170 (1990)

Molybdenum Carbide Catalysts

3. Turnover Rates for the Hydrogenolysis of *n*-Butane

J. S. LEE,[1] S. LOCATELLI,[2] S. T. OYAMA,[3] AND M. BOUDART[4]

Department of Chemical Engineering, Stanford University, Stanford, California 94305

Received December 7, 1988; revised March 21, 1990

The hydrogenolysis of *n*-butane was studied on Mo and Mo_2C supported on Al_2O_3 as well as on bulk carbides Mo_2C and α-MoC_{1-x}. Well-reduced molybdenum clusters supported on Al_2O_3 were prepared according to the method of Burwell and co-workers. The clusters were transformed in CH_4–H_2 mixtures into Mo_2C as shown by X-ray absorption spectroscopy. Turnover rates, v_t, referred to the number of surface metal atoms titrated by irreversible chemisorption of CO were very high both on supported and unsupported catalysts. The value of v_t for supported Mo_2C clusters was slightly less than that for Ru and Os, the most active metals known for the hydrogenolysis of alkanes. The reaction was found to be structure-sensitive since v_t values changed with particle size and crystal structure of catalysts. The presence of polymeric carbon on the surface, or possibly oxygen, and the structure sensitivity of the reaction seem responsible for the low v_t of unsupported Mo_2C reported previously. Molybdenum surfaces that were initially metallic transformed to carbides under reaction conditions, indicating that the active catalytic phase of metallic Mo was also Mo_2C.

INTRODUCTION

Turnover rates, v_t, for the hydrogenolysis of *n*-butane on unsupported Mo_2C powders were reported by two of us at the International Congress on Catalysis in Tokyo (*1*). In the discussion of this work, Burwell noted that the values of v_t obtained were more than two orders of magnitude smaller than those found in his laboratory for well-reduced molybdenum clusters supported on Al_2O_3 (*2*). The present work was initiated to understand the origin of this discrepancy.

Hexagonal Mo_2C and cubic α-MoC_{1-x} are prepared as unsupported powders with BET specific surface areas of close to 60 $m^2 g^{-1}$ and 200 $m^2 g^{-1}$, respectively, without appreciable surface contamination by carbon (*3*, *4*). The metallic molybdenum clusters supported on γ-alumina (Mo/Al_2O_3) are prepared according to the method of Burwell and co-workers (*5–9*). Carbided molybdenum clusters (Mo_2C/Al_2O_3) are prepared by treating those well-reduced metallic clusters with a CH_4/H_2 mixture. Samples are characterized by CO chemisorption, X-ray diffraction (XRD), X-ray absorption spectroscopy (XAS), and temperature-programmed reaction (TPR). This paper reports turnover rates for the hydrogenolysis of *n*-butane at 510 K and atmospheric pressure on these supported and unsupported catalysts.

EXPERIMENTAL

High-purity γ-alumina (99.99%, American Cyanamid, SN-5262) was used in the preparation of the supported samples. It had a BET specific surface area of 200 $m^2 g^{-1}$, a pore volume of 0.58 $cm^3 g^{-1}$, and impurities in wt% of $Na_2O < 0.002$, $SO_4 < 0.001$,

[1] Present address: Department of Chemical Engineering, Pohang Institute of Science and Technology, P.O. Box 125, Pohang, Kyungbuk 680, Korea.

[2] Present address: Universidad Nacional de Salta, Dpto. Ciencias Exactas, Calle Buenos Aires 177, 4400 Salta, Argentina.

[3] Present address: Department of Chemical Engineering, Clarkson University, Potsdam, New York 13676.

[4] To whom correspondence should be addressed.

0021-9517/90 $3.00

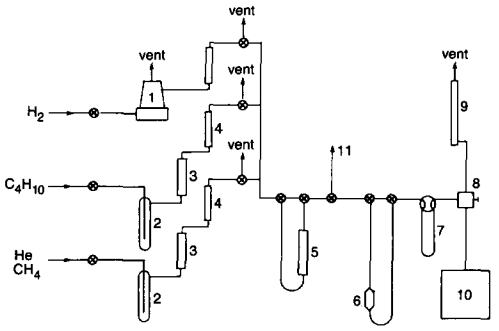

FIG. 1. Schematic of flow system. 1, Palladium thimble; 2, molecular sieve trap; 3, MnO/SiO_2 trap; 4, flow meter; 5, $Mo(CO)_6$ saturator; 6, quartz cell; 7, cold trap; 8, sample injection valve; 9, soap-film flow meter; 10, gas chromatograph; 11, vacuum line.

Fe < 0.004, and NiO, MoO_3, CoO < 0.001. Molybdenum hexacarbonyl $Mo(CO)_6$ (Alfa-Ventron) was purified by sublimation under vacuum. Molybdenum trioxide MoO_3 (Johnson Matthey, 99.998%) was used as received for the preparation of the unsupported samples. Dihydrogen (99.95%, Liquid Carbonic) was purified through a heated palladium cell. Helium (99.995%, Liquid Carbonic), methane (99.97%, Matheson) and *n*-butane (99.5%, Matheson) were purified through 5-Å molecular sieves and MnO/SiO_2 traps, both at room temperature (RT), The MnO/SiO_2 trap was activated in H_2 at 700 K prior to use (*10*). A flow system shown in Fig. 1 was used for sample preparation, reaction rate measurements, and temperature-programmed reaction (TPR). All experiments were carried out *in situ* without exposing samples to the atmosphere.

To prepare the supported samples, 0.1 g of 50/80 mesh γ-alumina was loaded in a 2-cm-diameter tubular quartz cell equipped with a coarse frit and dehydroxylated at 1160 K for 1 h in flowing He at a space velocity, SV, of 60,000 h^{-1}. Space velocity, SV, is defined as the volumetric flow rate of gas (STP) divided by the apparent sample volume. This treatment caused a 5% loss in surface area. Following dehydroxylation, the γ-alumina was cooled to 320 K or to 360 K. The $Mo(CO)_6$ was then sublimed onto the alumina by passing H_2 (SV = 100,000 h^{-1}) through a $Mo(CO)_6$ saturator kept at RT and over the alumina. The high space velocity assured sample homogeneity along the length of the bed. Samples with varying Mo loading were prepared by changing the time of exposure of the support to the saturated carrier gas. Following adsorption, the saturator was bypassed. The sample temperature was increased to 373 K under H_2 flow and maintained at 373 K for 1 h. Finally, the sample temperature was increased at the rate of 430 K h^{-1} to 970 K and maintained at this temperature for 1–3 h in flowing H_2. This preparation yielded reduced samples of Mo/Al_2O_3. Supported molybdenum carbide, Mo_2C/Al_2O_3, was prepared by subsequent carburization of these samples in a CH_4/H_2 mixture (15–20% CH_4, SV = 60,000 h^{-1}) between 930 and 980 K for 0.2–0.5 h, depending on Mo loading. Then the sample was treated in H_2 at 580 K until no CH_4 was detected at the reactor outlet. Values of Mo loading were determined by atomic absorption. Carbon content was determined by measuring CH_4 evolved during TPR with H_2.

Hexagonal Mo_2C powders were prepared by TPR of MoO_3 with a CH_4/H_2 mixture (20% CH_4, SV = 60,000 h^{-1}). The rate of heating from 670 to 920 K was 30 K h^{-1}. Cubic α-MoC_{1-x} (x = 0.5) powders were made in two steps. In the first step, molybdenum nitride, Mo_2N, powders with BET specific surface area, S_g, of ca. 200 m^2 g^{-1} were prepared by TPR between MoO_3 and ammonia (*11*). In the second step, Mo_2N powders were carburized by TPR with a 20% CH_4/H_2 mixture (*4, 12*). The product S_g was 190 m^2 g^{-1}. This sample is called α-MoC_{1-x}-H. To increase the particle size of MoC_{1-x}, the heating rate of the nitride preparation was raised from 30 to 100 K h^{-1}. The product S_g was then 120 m^2 g^{-1}. This sample is called α-MoC_{1-x} – M. A third sample was S_g equal to 20 m^2 g^{-1} was prepared by heating 190 m^2 g^{-1} nitride at 1000 K for 10 h in flowing N_2 prior to carburization. The

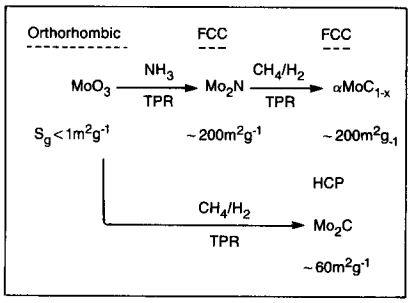

FIG. 2. Schematic procedures for the preparation of cubic α-MoC_{1-x} and hexagonal Mo_2C from MoO_3, their crystal structures, and BET specific surface areas (S_g).

resulting powder is called α-MoC_{1-x}-L. The procedures for the preparation of unsupported samples, their crystal structure, and S_g values are schematically represented in Fig. 2. The details of these solid transformations are described elsewhere (*3, 4, 11, 12*). Their properties are summarized in Table 1.

A sample of supported ruthenium (0.5% Ru/Al_2O_3) was obtained from Baker Co. in pellet form. The method of its preparation is unknown. It was crushed into a powder and reduced at 720 K for 2 h in flowing H_2 before adsorption and reaction rate measurements. An amount of 50 mg was used for reaction rate measurement.

TABLE 1

Properties of Unsupported Molybdenum Carbides

	Mo_2C	α-MoC_{1-x}-H	α-MoC_{1-x}-M	α-MoC_{1-x}-L
BET area ($m^2\ g^{-1}$)	60	190	120	20
Phase by XRD	Mo_2C	α-MoC_{1-x}	α-MoC_{1-x}	α-MoC_{1-x} Mo_2C
CO number density ($10^{15}\ cm^{-2}$)	0.22	0.26	0.36	0.33
D_p (nm by BET)[a]	11.0	3	5	32
D_c (nm by X-ray)[b]	11.5	5	9	10 (α-MoC_{1-x}) 80 (Mo_2C)

[a] $D_p = 6/\theta\ S_g$; θ is the density of the solid; S_g is the specific surface area by BET.

[b] $D_3 = \lambda/(\beta \cos \Theta)$; λ is the wavelength of X-ray radiation; Θ is the Bragg angle, β is the half-width corrected for $K\alpha$-doublet separation and instrumental broadening.

Chemisorption of CO was measured at RT in a constant-volume adsorption system (*13*). By isolating the cell with stopcocks, the sample was not exposed to air during transfer between the reactor and adsorption systems. Before chemisorption of CO, the sample was heated in H_2 at 570 K for 0.2 h, evacuated at this temperature for 0.5 h to 5 $\times\ 10^{-3}$ Pa, and then cooled to RT. An initial isotherm was taken to measure total CO uptake. Then the sample was evacuated at RT for 0.5 h to 5 $\times\ 10^{-3}$ Pa for 0.5 h and a second isotherm was obtained to measure weakly adsorbed CO. The isotherms were extrapolated to zero pressure and the difference in CO uptake at that pressure was taken as the amount of CO chemisorbed irreversibly. The alumina alone did not chemisorb CO.

All TPR experiments were carried out in H_2 flow (SV = 36,000 h^{-1}) using a heating rate of 430 K h^{-1} unless otherwise specified. The TPR results were obtained by analysis of gas products at temperature increments of 10 K, with the data interpolated to obtain smooth curves. Rates of hydrogenolysis of *n*-butane were measured in the same differential quartz reactor used for the preparations. Hydrogenolysis was carried out at 510 K and atmospheric pressure with a molar ratio of *n*-butane/H_2 of 0.11 to 0.25. The conversion of *n*-butane was less than 10% in all cases. Products of TPR and the reaction were analyzed with a gas chromatograph (HP 5980), equipped with thermal conductivity and flame ionization detectors, and connected to an integrator (HP 3600). A 2.5-m-long, 3-mm-diameter Chromosorb 102 column was used.

The X-ray diffraction (XRD) measurements were made on samples passivated with 1% O_2 in He at RT. Standard powder diffraction technique with Cu$K\alpha$ radiation was used. The X-ray absorption spectra (XAS) were obtained at the Stanford Synchrotron Radiation Laboratory (SSRL). Spectra at the Mo *K*-edge were taken of reduced and carburized samples with 3.1% Mo loading. These samples were prepared

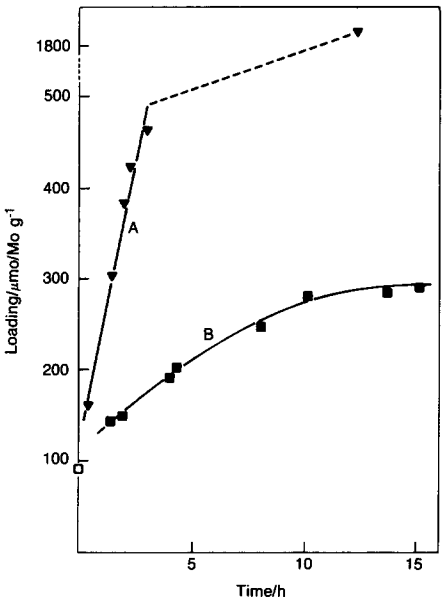

FIG. 3. Mo loading obtained when $Mo(CO)_6$ is adsorbed onto alumina at 360 K (curve A) and 320 K (curve B) as a function of time of exposure to $Mo(CO)_6/H_2$ flow. (□) Sample prepared by adsorption of $Mo(CO)_6$ under vacuum at RT.

by deposition of $Mo(CO)_6$ at 320 K with subsequent TPR with H_2 and carburization with a 20% CH_4/H_2 mixture. A 25-μm-thick Mo foil and Mo_2C powders with particle size of ca. 0.5 μm mixed with γ-alumina were used as references. The XAS data were collected at RT in an *in situ* quartz cell under the same gas atmosphere used during the sample preparation. The XAS data were analyzed as described in Ref (*14*).

RESULTS

Catalyst Preparation

In all preparations of supported samples, the rate of $Mo(CO)_6$ flow was 770 μmol h^{-1} per gram of alumina. This corresponded to the saturation concentration of $Mo(CO)_6$ in the gas carrier at room temperature (RT). Figure 3 shows the Mo loadings obtained plotted against the time of exposure to $Mo(CO)_6/H_2$ flow when the alumina was maintained at 360 K (curve A) and 320 K (curve B). At 320 K the adsorption of $Mo(CO)_6$ is a slow process. Samples with Mo loading greater than 200 Mo μmol g^{-1} required more than 5 h for preparation (100 Mo μmol g^{-1} = 0.94 wt%). The maximum Mo loading of 290 μmol Mo g^{-1} was obtained after 15 h in the $Mo(CO)_6/H_2$ flow. This corresponds to about a monolayer coverage of the γ-alumina by $Mo(CO)_6$. By monitoring CO evolution with a gas chromatograph during preparation, an average stoichiometry of $Mo(CO)_5$ was computed for the species adsorbed on the alumina surface. A sample was also prepared under static conditions by adsorption of $Mo(CO)_6$ at the vapor pressure of $Mo(CO)_6$ at RT, followed by evacuation at RT. This preparation gave a Mo loading of 90 μmol Mo g^{-1} (experimental point at zero time in Fig. 3). This corresponds to a strongly chemisorbed metal carbonyl on alumina. A similar value was reported by Kazusaka and Howe (*15*) for partially dehydroxylated γ-alumina. Samples with high Mo loading could be prepared rapidly at 360 K. Here, no upper limit to the $Mo(CO)_6$ adsorption was observed. An average stoichiometry of $Mo(CO)_{2-3}$ was computed for these species.

Following the adsorption of $Mo(CO)_6$ on the alumina, the temperature of the sample was increased at a rate of 430 K h^{-1} to 970 K in H_2 flow to decompose the molybdenum carbonyl species on the alumina surface. During the decomposition, CO and CH_4 were detected at the reactor outlet as shown in Fig. 4. The maxima of CO and CH_4 evolution were observed at 420 and 510 K, respectively. The CH evolution persisted above 900 K. All samples showed similar TPR profiles of CO and CH_4 evolution, regardless of preparation temperature used.

Subsequent treatment with a CH_4/H_2 mixture of the Mo/Al_2O_3 samples, prepared in the manner indicated above, resulted in carburized materials whose composition depended on the conditions of carburization. Figure 5 shows TPR spectra from a sample with an initial CO uptake of 520 μmol g^{-1} which was carburized under different conditions. Table 2 summarizes the conditions.

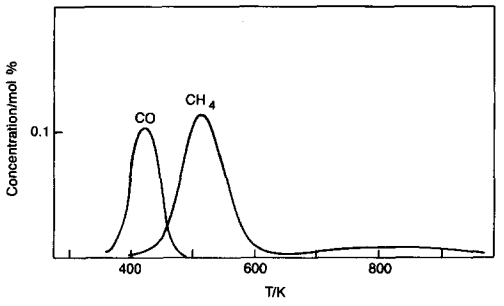

FIG. 4. A TPR profile of decomposition of $Mo(CO)_6/Al_2O_3$ in flowing H_2. The sample contained 270 μmol Mo g^{-1}. Heating rate was 430 K h^{-1}.

TABLE 2

Carburization Conditions for Mo/Al_2O_3

Run	T (K)	% CH_4 in CH_4/H_2 mixture	Carburization time (h)	C/Mo	CO/Mo
A	973	25	0.41	0.65	0.09
B	973	20	0.33	0.58	0.10
C	973	20	0.25	0.48	0.13
D	948	20	0.33	0.40	0.13
E	933	20	0.33	0.31	0.08

The peaks correspond to the removal of carbon by H_2 in the form of CH_4 and allow calculation of the C/Mo ratio. In all cases but one, the maximum temperature of TPR was limited to 980 K in order to avoid crystal growth of Mo. The samples were maintained at 980 K until no further CH_4 was detected. In the experiment corresponding to curve D, the TPR was extended to 1200 K, but no new peaks were observed. After a TPR, the sample was recarburized and a new TPR was carried out. After each carburization and before TPR, the sample was purged with H_2 and evacuated to 5×10^{-3} Pa at 573 K and the amount of chemisorbed CO was measured at RT.

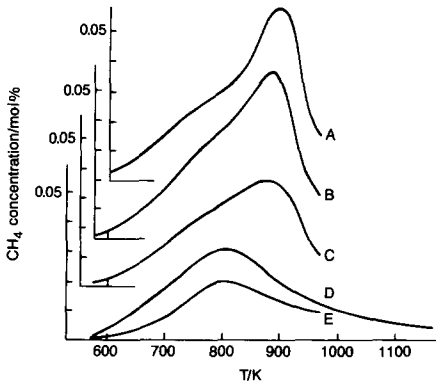

FIG. 5. The TPR profiles of carbon removal by H_2 from a sample containing 520 μmol Mo g^{-1} after carburization under different conditions. The heating rate was 430 K h^{-1}. Carburization condition, amount of carbon retained in the sample after carburization as determined by integration of peak area, and irreversible chemisorption of CO at RT after each carburization and before TPR are shown in Table 2.

The TPR data showed CH_4 peaks at 780 and 910 K. The first peak appeared in all samples and was assigned to the hydrogenation of carbidic carbon from Mo_2C. The second peak appeared only when the temperature of carburization was high or when a mixture with a high concentration of CH_4 had been used. This peak was assigned to the hydrogenolysis of polymeric carbon. Extreme carburization conditions, e.g., CH_4/H_2 mixtures of more than 30% CH_4 or synthesis temperatures above 980 K, yielded samples whose TPR profiles showed only one peak at 970–980 K. No peak around 780 K was observed; the polymeric carbon covered the surface completely. As a result of these experiments, to obtain samples free of polymeric carbon, carburization was carried out at 950 K with a 20% CH_4/H_2 mixture. During the repeated carburization/decarburization treatment described above, the amount of CO chemisorption on carburized samples did not change appreciably. This indicates that there was negligible crystal growth during this severe treatment.

XRD and XAS

The X-ray diffraction patterns of reduced or carburized supported samples with up to 7% loading showed no peaks corresponding to molybdenum or molybdenum carbide. On the other hand, the unsupported Mo_2C samples showed peaks corresponding to only

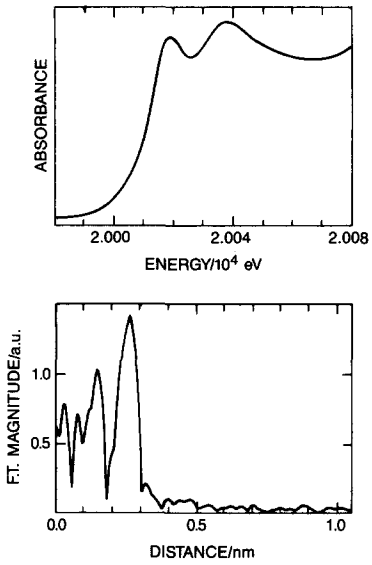

FIG. 6. XAE and RSF of $Mo(CO)_6/Al_2O_3$ prepared by $Mo(CO)_6$ adsorption at 320 K in flowing H_2. Peaks at 155 pm and at 266 pm correspond to Mo–C and Mo–O distances, respectively.

Mo_2C of the hexagonal close-packed (HCP) crystal structure with normal lattice parameters of a_0 = 299 pm and c_0 = 472 pm. The unsupported α-MoC_{1-x}-H and α-MoC_{1-x}-M XRD patterns revealed materials having the face-centered cubic (FCC) crystal structure with lattice parameters of 423 pm. The α-MoC_{1-x}-L was actually a mixture of cubic and hexagonal carbides. As shown in Table 1, the crystal sizes determined from full-width at half-maximum measurements of XRD line broadening were in good agreement with particle sizes estimated from BET specific surface area.

Plots of X-ray absorption spectra of $Mo(CO)_6/Al_2O_3$ prepared by adsorption of $Mo(CO)_6$ onto Al_2O_3 at 320 K are shown in Fig. 6. The top spectrum is the detailed structure of the X-ray absorption edge (XAE) near the Mo *K*-edge. A strong twin peak is characteristic of solid $Mo(CO)_6$ (*16*). The bottom spectrum is the Fourier transform of the extended X-ray absorption fine structure (EXAFS) of the Mo *K*-edge of the same sample. The Fourier transformation of an EXAFS spectrum results in a radial structure function (RSF). Major peaks in the RSF correspond to the important interatomic distances shifted from their true position by a phase shift (*17*). The peak heights at the same distance from the absorber are roughly proportional to the number of atoms at that distance if the thermal and static disorders of the atoms can be neglected. The RSF of $Mo(CO)_6/Al_2O_3$ in Fig. 6 is indistinguishable from the RSF of solid $Mo(CO)_6$ (*16*). Both show two peaks at distances of 155 pm for the Mo–C bond and of 266 pm for the Mo–O bond. Corresponding true distances are 206 pm for the Mo–C bond and 318 pm for the Mo–O bond (*16*). These peaks completely disappear on heating of $Mo(CO)_6/Al_2O_3$ to 370 K in H_2.

Figure 7 shows XAE spectra of a supported sample treated at increasing temperatures in flowing H_2. The spectra of a Mo foil and a Mo_2C powder mixed with γ-alumina were used as references. All the spectra showed identical edge position, defined as the first inflection point in the rapidly rising portion of the edge. This position was as-

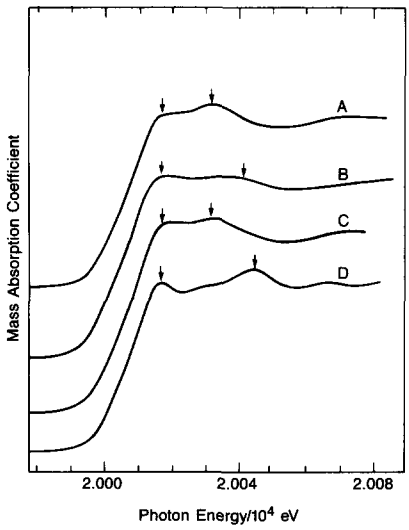

FIG. 7. XAE spectra of Mo/Al_2O_3 reduced by TPR with H_2 up to 930 K (A) and 970 K (B). The reference spectra of Mo_2C powder (C) and Mo foil (D) are also shown for comparison.

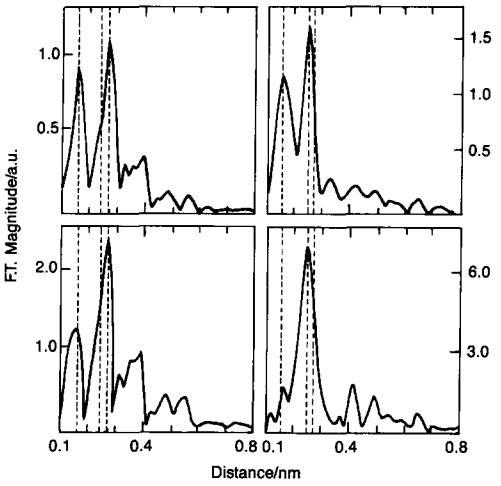

FIG. 8. RSF of Mo/Al_2O_3 reduced by TPR with H_2 up to 930 K (A) and 970 (B), and reference spectra of Mo_2C powder (C) and Mo foil (D).

signed an energy of 20003.9 eV. It is known that edge features move to higher energy as the oxidation state of Mo is raised (*16*). The only notable difference between Mo and Mo_2C XAE spectra was a separation of the two broad peaks above the absorption edge. The Mo foil spectrum (Fig. 7D) showed a larger separation than the Mo_2C spectrum (Fig. 7C). The XAE spectrum of the sample reduced in H_2 up to 930 K (Fig. 7A) was identical to the Mo_2C reference spectrum. When further reduced above 970 K (Fig. 7B), the sample showed an XAE spectrum which was more similar to the Mo foil spectrum.

The corresponding radial structure functions are shown in Fig. 8. The three dotted lines drawn vertically on each spectrum represent the Mo–C distance in Mo_2C (158 pm), the Mo–Mo distance in metallic Mo (238 pm), and the Mo–Mo distance in Mo_2C (262 pm), respectively. These distances should be corrected for phase shifts to get true distances. Using the known structure of the Mo and Mo_2C references, the phase shifts were determined to be 34 and 51 pm for Mo–Mo and Mo–C distances, respectively. The RSF of the sample reduced at 930 K (Fig. 8A) showed peaks at the same positions as those for the Mo_2C reference (Fig. 8C). With a further treatment with H_2 up to 970 K, the Mo–Mo peak position shifted to a shorter distance, but the Mo–C peak remained with negligible change in position (Fig. 8B). Only the sample treated to 1170 K showed the RSF characteristic of Mo (Fig. 8D).

In Fig. 9, the XAE and RSF of the sample obtained by carburization of Mo/Al_2O_3 reduced up to 970 K are compared with those of Mo_2C. The spectra of the two samples are identical in every detail except for the peak heights in the RSF.

The structural information abstracted from the RSF plots is tabulated in Table 3. Interatomic distances were obtained from the peak positions of the RSF and the experimentally determined phase shifts. The Mo–C and Mo–Mo coordination numbers were estimated from the heights of the peaks by comparison with the Mo_2C reference spectrum.

CO Chemisorption

Figure 10 shows the amount of CO chemisorbed irreversibly at RT, expressed as the ratio CO/Mo, as a function of Mo loading for

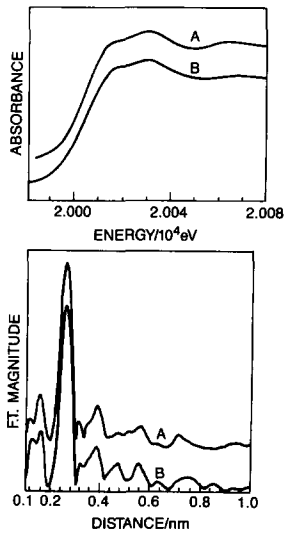

FIG. 9. XAE and RSF of Mo_2C powder (A) and Mo_2C/Al_2O_3 (B).

TABLE 3

Estimated Interatomic Distances and Coordination Numbers by XAS

Sample	Interatomic distance (pm)		Coordination number	
	Mo–C	Mo–Mo	Mo–C	Mo–Mo
Mo foil[a]	—	272	—	8
Mo_2C powder[a]	209	296	3	12
Mo/Al_2O_3, reduced up to 930 K	211	296	2	4
Mo/Al_2O_3, reduced up to 970 K	215	280	2	4
Mo_2C/Al_2O_3	211	296	2	6

[a] Structural data for Mo foil and Mo_2C powders were obtained from Refs. (*41*) and (*42*), respectively.

TABLE 4

Turnover Rates (v_t) of the Hydrogenolysis of *n*-butane

Catalyst	*n*-butane/H_2	v_t[a] 10^{-3} s^{-1}	Ref.
0.9% Mo/Al_2O_3	0.11	94	This work
1.0% Mo_2C/Al_2O_3	0.11	290	This work
2.7% Mo/Al_2O_3	0.25	14	This work
2.9% Mo/Al_2O_3	0.25	26	This work
Mo_2C	0.11	67	This work
α-MoC_{1-x}-H	0.11	8.6	This work
α-MoC_{1-x}-M	0.11	2.8	This work
α-MoC_{1-x}-M	0.11	4.1	This work
Mo_2C	0.11	0.08	*1*
0.8% Mo/Al_2O_3	0.04	160[b]	*2*
2.0% Os/Al_2O_3	0.11	450	*18*
Ru/Al_2O_3	0.11	820[b]	This work, (*19*)

[a] Turnover rates were based on surface metal atoms titrated by CO chemisorption at RT on a one-to-one basis before the reaction. The reaction was run at 510 K and under atmospheric pressure with conversions less than 10%.

[b] Extrapolated values (see text).

reduced and carburized supported samples. Slightly higher CO/Mo ratios were obtained for samples prepared at 320 K than for samples prepared at 360 K, perhaps due to the milder conditions used for the preparation of the former. The carburized samples chemisorbed more CO than the reduced samples. The results of CO chemisorption for unsupported samples are listed in Table 1 in terms of a number density, defined as the amount of CO chemisorbed per unit surface area. For the supported ruthenium a CO/Ru ratio of close to unity was obtained, suggesting that all the metal atoms were exposed to the surface.

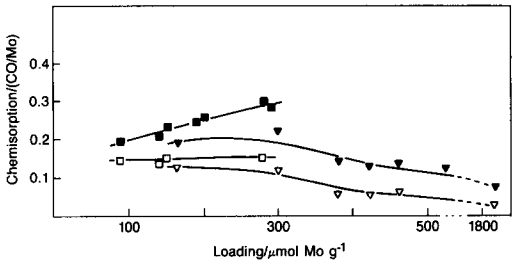

FIG. 10. Irreversible chemisorption of CO at RT expressed in CO/Mo ratio vs Mo loading: (□) Mo/Al_2O_3 by $Mo(CO)_6$ adsorption at 320 K; (■) Mo_2C/Al_2O_3 by $Mo(CO)_6$ adsorption at 320 K; (△) Mo/Al_2O_3 by $Mo(CO)_6$ adsorption at 360 K; (▲) Mo_2C/Al_2O_3 by $Mo(CO)_6$ adsorption at 360 K. The Mo/Al_2O_3 samples were reduced by TPR with H_2 up to 970 K.

Reaction Rate Measurement

The rates of *n*-butane hydrogenolysis for supported and unsupported molybdenum catalysts are reported in Table 4. The rate is expressed as a turnover rate, v_t, defined as the number of *n*-butane molecules converted to products per CO-titrated surface metal atoms per second. Each chemisorbed CO molecule was assumed to titrate one surface metal atom. All samples showed a 30–50% decrease in activity from initial rates during the first 0.2 h on stream, after which the deactivation was slow enough to allow steady-state rates to be measured.

The rate on the 0.5% Ru/Al_2O_3 sample was measured in the same manner as that on the molybdenum catalysts (Table 4). Again the rate is referred to the number of surface atoms titrated by CO.

Table 4 also shows the extrapolated v_t from the study of Nakamura *et al.* (*2*). They reported a rate of propane hydrogenolysis of 0.067 s^{-1} on Mo/Al_2O_3 (based on total molybdenum atoms at 523 K and atmospheric pressure with a H_2/C_3H_8 molar ratio of 24). This catalyst was prepared by a method similar to that used here for the preparation of reduced catalysts. They found that hydrogenolysis of *n*-butane proceeded 1.2 times faster than hydrogenolysis of propane in a pulse reactor. The v_t value in Table 3 was calculated using this information and their estimate of 30% metal exposed. The temperature difference was corrected by means of an activation energy of 80 kJ mol^{-1} obtained for the Mo/Al_2O_3 samples in the present study. The rate on Os was obtained from the work of Betizeau *et al.* (*18*). The v_t of unsupported Mo_2C from the previous work of Boudart *et al.* (*1*) was two to three orders of magnitude smaller than those for the other molybdenum and molybdenum carbide catalysts.

Phase Change in the Mo/Al_2O_3 Catalyst during Reaction

A sample of the Mo/Al_2O_3 catalyst undergoing hydrogenolysis of *n*-butane at 510 K and under atmospheric pressure was studied by XAE. The XAE spectra were taken by interrupting the reaction at different stages and cooling the samples to RT under the same reactive gas atmosphere. The fresh Mo/Al_2O_3 (Fig. 11B) showed the large separation between two broad peaks above the absorption edge characteristic of metallic Mo (Fig. 11A). In the XAE spectrum collected after 4 h of the reaction (Fig. 11C), the high-energy peak shifted closer to the low-energy peak, thus making the spectrum more similar to that of the Mo_2C reference (Fig. 11F). No further changes were observed in XAE spectra taken after 12 h of the reaction (Fig. 11D). After carburization (Fig. 11E), the XAE spectrum of the catalyst became identical to that of the Mo_2C reference spectrum. The change in RSF was not appreciable within the reliability of the technique, i.e., 2 pm in the determination of interatomic distances and 20% in the estimation of coordination numbers (*16*).

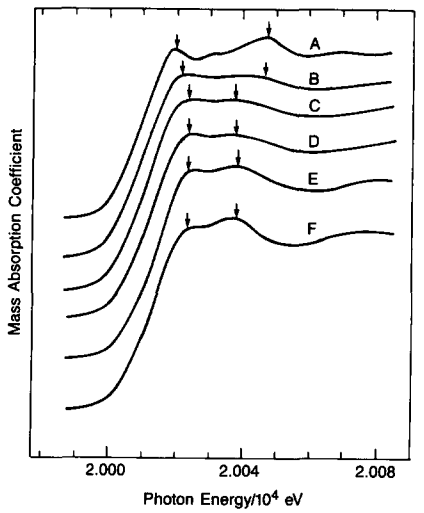

FIG. 11. The change in XAE spectra of Mo/Al_2O_3 during *n*-butane hydrogenolysis at 510 K, atmospheric pressure, and $4H_2$/*n*-butane: (A) Mo foil; (B) fresh Mo/Al_2O_3; (C) Mo/Al_2O_3 after 4 h of the reaction; (D) Mo/Al_2O_3 after 12 h of the reaction; (E) after carburization (Mo_2C/Al_2O_3); (F) Mo_2C powder.

DISCUSSION

Preparation and Characterization of Catalysts

The process of adsorption and decomposition of $Mo(CO)_6$ on alumina is complex. At least three different subcarbonyl species [$Mo(CO)_x$, x = 3, 4, and 5] have been identified or untreated or partially dehydroxylated alumina by heating adsorbed $Mo(CO)_6$ below 370 K (*5*). However, unlike on partially dehydroxylated alumina, on dehydroxylated alumina the liberation of CO was not discrete (*9*). Our $Mo(CO)_6/Al_2O_3$ sample, prepared by adsorption of $Mo(CO)_6$ at 320 K onto dehydroxylated γ-alumina, exhibits an XAS spectrum indistinguishable from that of solid $Mo(CO)_6$. The structure of the adsorbed carbonyl species is similar to that of solid $Mo(CO)_6$, even though the adsorbed species has lost one CO ligand, on the average, by adsorption. This is the reason that

the Mo loading attainable from adsorption of $Mo(CO)_6$ on γ-alumina at 320 K is limited to one monolayer. On the other hand, the $Mo(CO)_6$ structure is destroyed if adsorption is carried out at 360 K and there is no limit to the Mo loading at this temperature. The features of the XAS spectrum characteristic of $Mo(CO)_6$ completely disappear when $Mo(CO)_6/Al_2O_3$ prepared at 320 K is heated to 370 K, confirming the decomposition of the carbonyl species.

The decomposition process is complicated by the formation of a carbide phase even in H_2. Both XAE and RSF indicate that Mo_2C is formed at around 930 K. The carbide is probably formed as the $Mo(CO)_5$ species decompose to form clusters of molybdenum. During this process most of the carbon from the CO ligands is removed as methane but a part is incorporated as carbide. Other evidence of carbide formation can be seen in the TPR profile of $Mo(CO)_6/Al_2O_3$ decomposition in H_2 (Fig. 4). The broad CH_4 peak around 800 K coincides with the peak position of carbidic carbon in the TPR profile of the carburized sample (Fig. 5). From the peak area, the amount of carbon retained by this sample was estimated to be 0.1–0.2 carbon atoms per Mo atom (C/Mo). Thus the material in this sample is highly carbon-deficient. The surface layer appears to be completely free of carbon since the CO chemisorption behavior of this sample is identical to that of Mo/Al_2O_3 reduced up to 970 K, but completely different from that of Mo_2C/Al_2O_3 (see below). Badad-Zakhryapin *et al.* (*20*) also observed highly carbon-deficient carbides in coatings formed by the decomposition of tungsten and molybdenum carbonyls in H_2 at 670–770 K.

Further treatment up to higher temperatures substantially destroys the carbide structure. The XAE spectrum of the sample treated up to 970 K approaches that of metallic Mo (Fig. 7B). However, a small amount of carbon still remained in this sample since the Mo–C peak in the RSF does not disappear (Fig. 8B). Also, the position of the Mo–Mo peak lies between the positions expected for metallic Mo and Mo_2C. Only the sample treated up to 1170 K showed XAS spectra with all the features of metallic Mo. The amount of carbon retained in the sample treated up to 970 K was determined to be 0.01 C/Mo by measuring the methane peak area produced from TPR with H_2 up to 1170 K. A similar value was also obtained by Nakamura *et al.* (*2*) using the same method of analysis for their Mo/Al_2O_3. This amount of carbon is too small to account for the substantial disturbance of the structure of the Mo clusters, but at these low levels of carbon the concentration is difficult to determine accurately and it is likely that the carbon content is underestimated. Because of the small size of these clusters, even small amounts of carbon might be enough to disturb the structure of Mo clusters. Molybdenum is known not to dissolve carbon in its lattice without forming carbide (*21*). Another possibility is that oxygen is incompletely removed by the reduction and remains in the structure together with carbon. Thus, Mo/Al_2O_3 reduced up to 970 K is essentially metallic Mo with a carbide or perhaps oxycarbide impurity phase. All CO chemisorption and reaction rates are measured on this well-reduced sample. Upon carburization with a CH_4/H_2 mixture, well-reduced Mo clusters in Mo/Al_2O_3 readily transform to Mo_2C as shown by XAS.

The XAS also indicates that the average metal coordination numbers of Mo and Mo_2C clusters are about half of those in the bulk Mo and Mo_2C (Table 3). The absolute values of these numbers are imprecise, since they were not corrected for disorder effects (*17, 22*). However, greatly reduced coordination numbers for supported samples relative to corresponding bulk values and the fact that no XRD peaks of molybdenum compounds were found indicate that the Mo and Mo_2C in the sample are in the form of small particles.

The XAE spectra in Fig. 6 show that the catalyst samples, metallic Mo, and Mo_2C have identical edge positions. This suggests

that the molybdenum species in all our samples have an oxidation number near zero. Previous XPS work of Ramqvist (*23*) suggests a charge transfer from metal to carbon when metal carbide is formed. This effect does not seem large enough to move the edge position appreciably. However, the shift in binding energy observed by XPS may be caused by suppressed screening when going from Mo to MoC_2. With less mobile electrons there is less screening and this simulates a positive charge. The complete reduction of molybdenum is probably achieved because of the use of a dehydroxylated γ-alumina support. Oxidation of Mo occurs when $Mo(CO)_6/Al_2O_3$ is adsorbed on partially dehydroxylated alumina and is decomposed above 570 K (*7, 9*).

Irreversible chemisorption of CO at RT was used to count the number of surface metal atoms for the supported and unsupported catalysts. It is well known that metallic molybdenum completely dissociates CO at RT (*24*). By depositing a monolayer of carbidic carbon on the Mo(100) surface, Ko and Madix (*25*) observed that dissociative chemisorption of CO was completely suppressed. But this carburized Mo(100) surface still chemisorbed a monolayer of molecular CO. A monolayer was defined as one CO per surface molybdenum atom. Our chemisorption results on supported catalysts are in good agreement with these results on single crystals; the carburized samples chemisorb about twice as much CO as the reduced samples.

Turnover Rates of n-Butane Hydrogenolysis

The 0.9% Mo/Al_2O_3 used in this study (Table 4) reproduces the high v_t reported by Nakamura *et al.* (*2*). Furthermore, a considerable improvement is achieved by carburization of the same catalyst. Unsupported molybdenum carbides also show v_t values as high as those for supported catalysts. The v_t values of our Mo-containing catalysts are all very high and comparable to those on active Group 8 metals (Table 3). The v_t for 1.0% Mo_2C/Al_2O_3 is only slightly less than those for Os and Ru, the two most active metals for hydrogenolysis of alkanes. The hydrogenolysis of *n*-butane on ruthenium has been studied by many investigators (*26–33*). The reaction has generally been studied at lower temperatures than those employed here. In order to avoid extrapolation of rate data over widely differing conditions of total and partial pressure and temperature, the rate on a supported ruthenium catalyst was measured at the conditions used in this study.

All values of v_t of the supported and unsupported molybdenum catalysts are at least two orders of magnitude higher than the v_t for unsupported Mo_2C reported previously by Boudart *et al.* (*1*). The previous less active Mo_2C, with a C/Mo atomic ratio of 0.9, contained much more carbon than expected from the stoichiometry. It did not chemisorb H_2 and only 2% of the total surface chemisorbed CO. Furthermore, the presence of polymeric carbon on its surface was evidenced by Auger electron spectroscopy. Thus, the lower value of v_t reported previously is probably due to polymeric carbon covering part of the surface of the Mo_2C used in that study. Again, we cannot rule out the presence of a small amount of oxygen in addition to the carbon. Regardless of the elemental nature of the surface contaminant, the magnitude of the rate difference is too large to be accounted for by simple site blockage because the v_t values are referred to the number of surface atoms titrated by CO chemisorption which does not count contaminated surface atoms. Thus, another explanation is necessary.

The hydrogenolysis of alkanes is known to be a structure-sensitive reaction. The most convincing evidence may be found in the recent work of Goodman (*33, 34*) which showed that the turnover rates of hydrogenolysis of ethane and *n*-butane were more than one order of magnitude higher on Ni(100) than on Ni(111). They were also shown to be strongly dependent on particle size of supported catalysts (*35, 36*). In this

work the v_t values of *n*-butane hydrogenolysis on Mo/Al_2O_3 and Mo_2C/Al_2O_3 increase by a factor of 10 by reducing the Mo loading from 2.7 to 0.9%. This agrees both in direction and in magnitude with the effect observed for Group 8 metals (*31, 36*). Thus, the catalysts with low Mo loading, which probably contain smaller clusters of Mo or Mo_2C, exhibit higher rates of hydrogenolysis than the catalysts with high Mo loading, which contain larger clusters. The availability of unsupported powders of molybdenum carbides of different crystal structure with sizes in the range of 3–10 nm provides a better opportunity for checking the structure sensitivity of the reaction. Here, there is no fear of any type of support effect making the influence of particle size equivocal. As shown in Table 4, the v_t of hexagonal Mo_2C is higher than those of cubic α-MoC_{1-x}. It is shown elsewhere (*37*) that the lower v_t for α-MoC_{1-x} is not due to gas-phase mass transfer limitations. Also, smaller α-MoC_{1-x} particles show higher v_t than larger ones. Thus, as is the case with Group 8 metals, the hydrogenolysis of *n*-butane on molybdenum carbide is a structure-sensitive reaction with v_t varying with particle size and crystal structure.

If structure sensitivity of the hydrogenolysis relates to the need for large ensembles of sites (*38*), the sharp decrease in v_t caused by polymeric carbon, or possibly oxygen, can be understood. Polymeric carbon or oxygen destroys ensembles which are required for the reaction. This effect is not accounted for by CO chemisorption since CO counts individual sites rather than ensembles. It should be noted that this effect of polymeric carbon for the hydrogenolysis of *n*-butane is very similar to the effect observed when an inactive metal like Cu, Au, or Ag is alloyed with an active metal like Ni, Pt, or Pd for various hydrocarbon–H_2 reactions (*31, 38*). In addition to drastic changes in selectivity, the rates of hydrogenolysis of alkanes per active metal atom were strongly suppressed, by one to two orders of magnitude, as an inactive component was added. This effect also has been interpreted as inactive metal atoms destroying ensembles of active metal atoms required for the hydrogenolysis.

The v_t values for Mo_2C/Al_2O_3 are only two to three times higher than those for Mo/Al_2O_3. The activation energy and product distribution reported elsewhere (*37*) are indistinguishable from each other. The XAE spectra in Fig. 11 collected during the reaction indicate a phase change of Mo in the Mo/Al_2O_3 catalyst. Thus, well-reduced molybdenum transforms to molybdenum carbide as soon as the reaction mixture is introduced. The active catalytic phase of metallic molybdenum is, therefore, also molybdenum carbide. The two to three times lower rates of initially metallic catalysts compared to those of precarburized catalysts are probably due to deposition of polymeric carbon during the reaction which occurs simultaneously with carbide formation. The balance between these two processes is very sensitive to the carburizing gas and the carburization conditions (*3*). The formation of carbide on these supported catalysts during hydrogenolysis seems limited to the surface layers. The XAE spectra of Mo/Al_2O_3 during the reaction show mixed features of both fresh Mo/Al_2O_3 and Mo_2C/Al_2O_3. There was also little appreciable change in the RSF. On unsupported molybdenum Sinfelt and Yates (*39*) reported that metallic molybdenum underwent bulk carburization as the hydrogenolysis of ethane was carried out. The reaction reached a steady state well before bulk carburization occurred. In a study of the surface properties of molybdenum catalysts (*40*), a surface nitride of molybdenum was shown to exhibit the catalytic behavior of bulk nitride even though only the topmost two layers were nitrided. Thus only the surface layers are involved in the catalysis.

Finally, we would like to point out that although the rate of hydrogenolysis in this work agrees with that reported before by Burwell and co-workers, we still find a disagreement in the rate of isomerization (formation of *i*-butane). In the present work, the

rate of isomerization is 4 to 10% of the total rate, while Burwell and co-workers reported no isomerization of *n*-butane (*2*). This difference might be due to the presence in our case of oxygen on the surface, as will be reported in detail later (*43*).

CONCLUSIONS

(1) Supported and unsupported molybdenum carbide catalysts have turnover rates for *n*-butane hydrogenolysis comparable to the most active transition metal catalysts.

(2) Both catalyst crystallographic structure and particle size significantly affect the catalyst activity, indicating that the reaction is structure-sensitive.

(3) Initially metallic molybdenum surfaces transform to carbides under reaction conditions, indicating that the active phase of metallic Mo is Mo_2C.

ACKNOWLEDGMENTS

This work was supported by NSF Grant NSF-CPE-82-19066 and NSF through the Center for Materials Research at Stanford. The XAS experiments were performed at the Stanford Synchrotron Radiation Laboratory, which is supported by the Department of Energy (Division of Materials Research), the National Science Foundation (Division of Materials Research), and National Institute of Health (Biotechnology Resource Program, Division of Health Resources).

REFERENCES

1. Boudart, M., Oyama, S. T., and Leclercq, L., *in* "Proceedings, 7th International Congress on Catalysis, Tokyo, 1980 (T. Seiyama and K. Tanabe, Eds.), Vol. 1, p. 578. Elsevier, Amsterdam, 1980.
2. Nakamura, R., Bowman, R. G., and Burwell, R. L., Jr., *J. Amer. Chem. Soc.* **103,** 673 (1981).
3. Lee, J. S., Oyama, S. T., and Boudart, M., *J. Catal.* **106,** 125 (1987).
4. Lee, J. S., Volpe, L., Ribeiro, F., and Boudart, M., submitted for publication.
5. Brenner, A., and Burwell, R. L., Jr., *J. Amer. Chem. Soc.* **97,** 2566 (1975).
6. Burwell, R. L., Jr., and Brenner, A., *J. Mol. Catal.* **1,** 77 (1975/1976).
7. Brenner, A., and Burwell, R. L., Jr., *J. Catal.* **52,** 353 (1978).
8. Brenner, A., and Burwell, R. L., Jr., *J. Catal.* **52,** 364 (1978).
9. Bowman, R. G., and Burwell, R. L., Jr., *J. Catal.* **63,** 463 (1980).
10. McIlwrick, C. R., and Phillips, C. S. C., *J. Phys. E* **6,** 1208 (1973).
11. Volpe, L., and Boudart, M., *J. Solid State Chem.* **59,** 332 (1985).
12. Volpe, L., and Boudart, M., *J. Solid State Chem.* **59,** 348 (1985).
13. Hanson, F. V., PhD dissertion, Stanford University, 1975.
14. Weber, R. S., PhD dissertation, Stanford University, 1983.
15. Kazusaka, A., and Howe, R. F., *J. Mol. Catal.* **9,** 183 (1980).
16. Cramer, S. P., Eccles, T. K., Kutzler, F. W., Hodgson, K. O., and Mortenson, L. E., *J. Amer. Chem. Soc.* **98,** 1287 (1976).
17. Stern, E., Sayers, D., and Lytle, F. W., *Phys. Rev. B* **11,** 4836 (1975).
18. Betizeau, C., Leclercq, G., Maurel, R., Bolivar, C., Charcosset, H., Frety, R., and Tournayan, L., *J. Catal.* **45,** 179 (1976).
19. Sinfelt, J. H., *in* "Advances in Catalysis" (D. D. Eley, H. Pines, and P. B. Weisz, Eds.), *Adv. Catal.* Vol. 23, p. 91. Academic Press, San Diego, 1976.
20. Badad-Zekhryapin, A. A., Lysenko, L. T., and Gert, L. M., *Fiz. Met. Metalloved.* **21,** 782 (1966).
21. Rudy, E., Windisch, S., Stosick, A. J., and Hoffman, J. R., *Trans. TMS-AIME* **239,** 1247 (1967).
22. Eisenberger, P., and Brown, G. S., *Solid State Commun.* **29,** 481 (1979).
23. Ramqvist, L., *J. Appl. Phys.* **42,** 2113 (1971).
24. Felter, T. E., and Estrup, P. J., *Surf. Sci.* **54,** 179 (1976).
25. Ko, E. I., and Madix, R. J., *Surf. Sci.* **109,** 221 (1981).
26. Kempling, J. C., and Anderson, R. B., *Ind. Eng. Chem. Process Des. Dev.* **11,** 146 (1972).
27. Nazimek, D., *React. Kinet. Catal. Lett.* **13,** 155 (1980).
28. Delmon, J. A., and Martin, G. A., *J. Catal.* **66,** 214 (1980).
29. Bond, G. C., and Yide, X., *J. Chem. Soc. Chem. Commun.,* 1248 (1983).
30. Sarkany, A., Matusek, K., and Tetenyi, P., *J. Chem. Soc. Faraday Trans. 1* **80,** 1699 (1984).
31. Bond, G. C., and Yide, X., *J. Mol. Catal.* **25,** 141 (1984).
32. Bond, G. C., and Yide, X., *J. Chem. Soc. Faraday Trans. 1* **80,** 3103 (1984).
33. Goodman, D. W., *Surf. Sci.* **123,** L679 (1982).
34. Goodman, D. W., *in* "Proceedings, 8th International Congress on Catalysis, Berlin, 1984," Vol. 4, p. 3. 1984 [preprint].
35. Yates, D. J. C., and Sinfelt, J. H., *J. Catal.* **8,** 348 (1967).
36. Maurel, R., Leclercq, G., and Trochet, J., *C.R. Seances Acad. Sci. Ser. C* **276,** 1353 (1973).
37. Lee, J. S., and Boudart, M., submitted for publication.

38. Ponec, V., *in* "Advances in Catalysis" (D. D. Eley, H. Pines, and P. B. Weisz, Eds.), Vol. 32, p. 149. Academic Press, San Diego, 1983.
39. Sinfelt, J. H., and Yates, D. J. C., *Nat. Phys. Sci.* **229,** 27 (1971).
40. Boudart, M., and Oyama, S. T., *J. Res. Inst. Catal. Hokkaido Univ.* **28,** 305 (1980).
41. Swanson, H. E., and Tatge, E., *U.S. Bur. Stand. J. Research* **46,** 318 (1951).
42. Parthé, E., and Sadagopan, V., *Acta Crystallogr.* **16,** 202 (1963).
43. Raffeis, G., Ribeiro, F. H., and Boudart, M., to be published.